Rotating flow instability prediction using eigenvalue analysis

Shenren Xu [*][1]

[1]*School of Power and Energy, Northwestern Polytechnical University, Xi'an, 710072, China*

The compression system in turbomachines, e.g., aircraft engines and gas turbines, when operating under off-design conditions, exhibits self-excited unsteady phenomena such as surge, rotating stall and rotating instability, leading to performance deterioration and/or structural damages. Inability to accurately predict when such flow instability occurs limits the development of high performance compression system. In this paper, an eigenvalue problem is solver to (1) predict the linear stability and (2) find the destabilizing eigenmode for a classical commonly seen for turbomachines operating at near stall conditions. The eigenvalue analysis is fully based on the steady state three-dimensional Reynods-averaged Navier-Stokes equations and thus the stability boundary is fully consistent with the one that is predicted by the time-accurate flow simulation, i.e., URANS, but two to three times faster. The method is applied to the computation of stability boundary of (i) the laminar flow around a two-dimensional circular cylinder, (ii) the flow around a quasi-three-dimensional compressor anuular cascade, and (iii) flow around a three-dimensional compressor rotor. The method developed here has the potential to revive the once-popular eigenvalue method for prediction rotating stall and surge, which was based on lower-fidelity flow models and provide industry with tools to accurately predict the stall line in the early design stage.

I. The nonlinear flow solver

A. Governing equations

B. Spatial discretization

II. Global linear stability analysis

For a nonlinear dynamic system, e.g., the discretised NS equation, using the method of lines, the governing equation is

$$\frac{d\mathbf{u}}{dt} = -\mathbf{R}(\mathbf{u}) \tag{1}$$

where $\mathbf{u}$ is the time-varying flow variable and $\mathbf{R}(\mathbf{u})$ is the nonlinear residual representing the spatial discretization. Assuming a steady state solution $\mathbf{u}_0$ (equilibrium point of the dynamic system) exists, and the time-varying flwo variable

---

*Corresponding author, email address: shenren_xu@nwpu.edu.cn

can be decomposed as the steady and the unsteady part

$$\mathbf{u} := \mathbf{u}_0 + \tilde{\mathbf{u}} \tag{2}$$

and the governing equation becomes

$$\frac{d\tilde{\mathbf{u}}}{dt} = A\tilde{\mathbf{u}} \tag{3}$$

where A is the negative Jacobian $A := -\dfrac{\partial \mathbf{R}}{\partial \mathbf{u}}$.

In order to use the eigen model decomposition approach, suppose the system matrix has right eigenvectors $\{\mathbf{v}_i, \mathbf{v}_2, ..., \mathbf{v}_N\}$, which forms the matrix V as its colum vectors. Matrix A can then be factorized as

$$A = V\Lambda V^{-1} \tag{4}$$

where the diagonal matrix Λ has the eigenvalues on the matrix A as its diagonal elements. Decomposing the unsteady part $\tilde{\mathbf{u}}$ in the eigen modal space, it can be expressed as a linear combination of all eigenvectors with coordinates η

$$\tilde{\mathbf{u}} = V\eta \tag{5}$$

Substituting the $\tilde{\mathbf{u}}$ in the governing equation using the eigen modal decomposition, it becomes

$$\frac{d\eta}{dt} = \Lambda\eta \tag{6}$$

Different from the original coupled system, all variables are decoupled now and it can be written as

$$\frac{d\eta_i}{dt} = \lambda_i\eta_i \quad \forall i \tag{7}$$

For the linear system to be stable, the sufficient and necessary condition is that all eigenvalues has a negative real part, i.e., real(λ_i), $\forall i$.

A. Numerical implementation

In practice, performing the global linear stability analysis as described above is a standard procedure involving three steps:

- Find an equilirium point (converging to steady state solution);
- Linearize the nonlinear residual and form the Jacobian matrix;
- Calculate the eigenvalue with the largest real part.

B. Time-domain unsteady approach

C. Eigenvalue approach

## III. Eigenvalue analysis for large sparse matrices

IV. Results

A. Laminar flow around a two-dimensional circular cylinder

Eigenvalue analysis is performed for the canonical case of the laminar flow around a circular cylinder with the Reynolds number in the range between 40 and 100. The computational domain is a circular cylinder centered at the origin with a diameter of $D = 10^{-5}$ and the farfield is a circle with a diameter of $100D$. The left half of the outer circle is set to 'farfield' boundary condition with a incoming flow of Mach 0.2 in the x-direction, a static pressure of 101325 Pa and and a temperature of 288.15 K. The right half ot he circle is set to 'pressure-outlet' boundary condition, with a constant pressure of 101325 Pa. The computational domain is meshed with quadrilateral elements, with a total of 29600 grid points. The density is 1.225 kg/m^3. The dynamic viscosity is varied in order to achieve a particular Reynolds number.

1. Steady state calculation

The steady state flow is obtained by either using an implicit solution method in Fluent (version 19.2) or by resorting to the Newton-Krylov algorithm in NutsCFD, despite the fact that the flow is physically unsteady under this condition. The Mach number contour of the NutsCFD calculation is shown in Fig. 1.
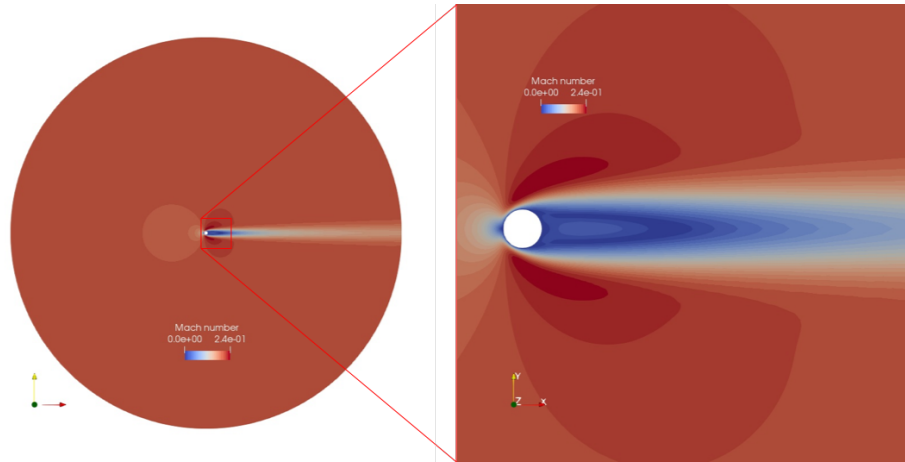
Fig. 1   Mach number contour plot of the calculation results by NutsCFD for Re = 55.

To compare the Fluent and NutsCFD results quantitatively, the velocity-x behind the cylinder as well as the pressure coefficient along the cylinder surface are compared in Fig. 2 and very good agreement can be found.
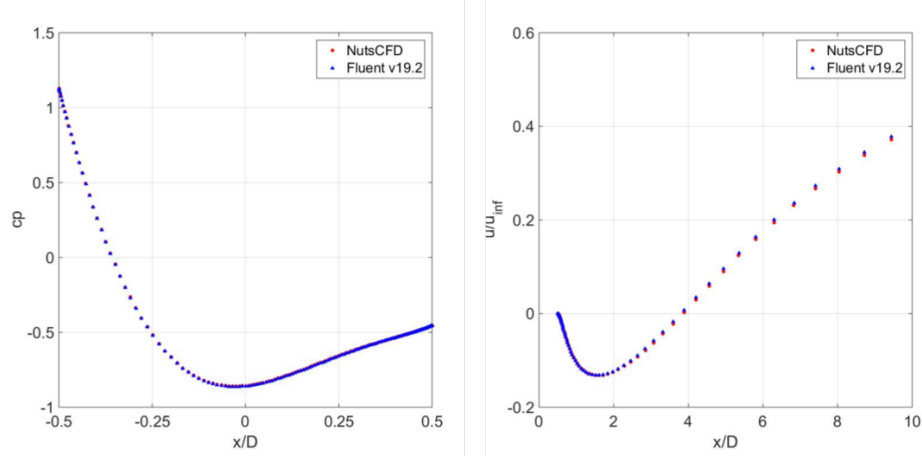
Fig. 2   Comparison between Fluent and NutsCFD calculation results for velocity-x along the center line behind the cylinder (left) and pressure coefficient along the cylinder surface (right).

2. Unsteady calculation

Experimental results show that the laminar flow around the cylinder becomes unsteady for Re above a critical value (around 47). To study this phenomenon, unsteady flow calculation for $Re = 55$ and $Re = 40$ are performed using Fluent. First, for both conditions, a steady state flow solution is obtained by converged the residual to machine error. For $Re = 55$, the unsteady simulation is run with the steady state as initial condition. A BDF2 second-order implicit dual-time-stepping method is used with the physical time step set to $10^{-8}sec$, that is, $0.01ms$, and the inner loop is solved with a CFL of 1000 and maximum 5 iterations. Roughly two orders of magnitude of residual drop is achieved for the inner loop. From Fig. 3, it can be seen that after around $100ms$, the lift coefficient starts to grow and eventually reaches a saturated limit cycle at around $130ms$. On the contrary, running unsteady simulation with a fully converged steady state for $Re = 40$ does not lead to unsteadiness. To probe the flow at $Re = 40$ further, a disturbance is introduced into the flow from the farfield by setting the incoming flow direction to vertical for one time step and switching it back to the horizontal direction, and then continue the unsteady run. The lift coefficient shows a transient response but eventually slowly delays to zero. These two sets of lift coefficient signals are plotted in Fig. 3 in both linear and logrithm scales. The logrithmic plot on the right clearly shows an exponential growth and decay for $Re = 55$ and $Re = 40$, respectively.

The growth and decay rate for both conditions can be extracted from the time signal and then be compared to the eigenvalue analysis results.

The same unsteady simulation is not performed in NutsCFD as the code is slower than fluent and in the meantime, it is believed that the unsteady response between the two solvers will be very similar, based on the comparison of the steady state solutions.
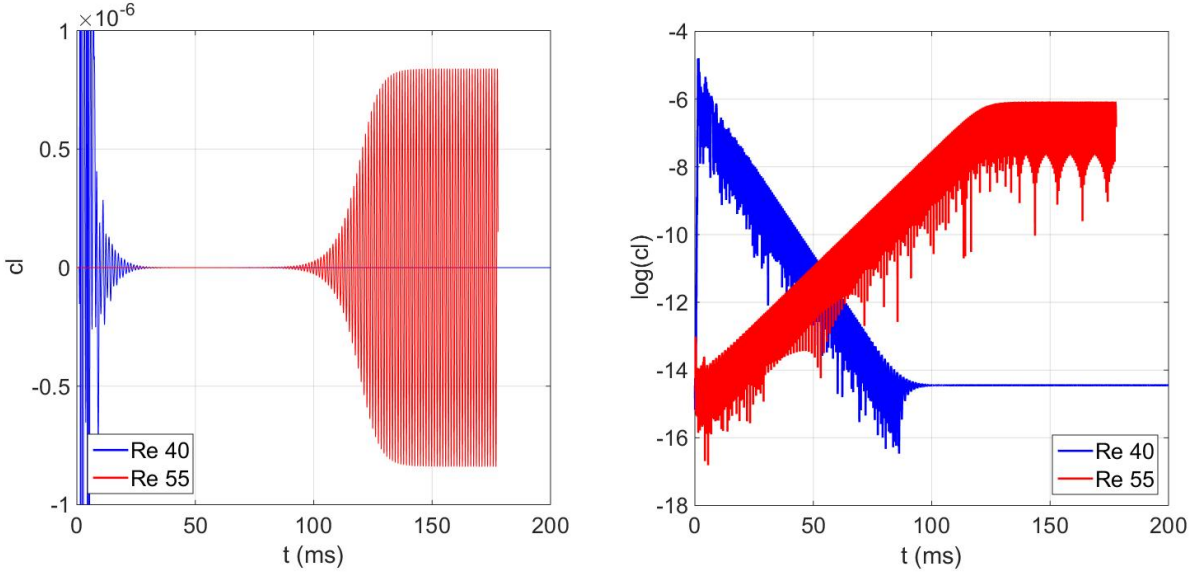
**Fig. 3   Lift coeffient histogram for Re = 55 and Re = 40.**

3. Eigenvalue analysis

An eigenvalue analysis is performed for the steady state solution calculated in NutsCFD. After converging the steady state solver to machine error ($tol = 10^{-14}$), the exact Jacobian matrix based on the 2nd-order spatial accuracy is calculated and output to file. The sparse matrix is read into Matlab and eigs is used to compute a subset of the eigenvalues, with the aim of finding the (hopefully one) unstable mode. To minimize the computational effort, 10 eigenvalues/vectors are computed for matrices with different shifts of 0, i, $2i$, $3i$, $4i$, $5i$. All the eigenvalues, 60 in total and with some duplicated, are plotted in Fig. 4. It can be seen that there is one eigenvalue that is on the right side of the imaginary axis, indicating there is one unstable mode. In the meantime, from the time-domain simulation, one can extract from the lift-coefficient signal that the flow is linearly growing with a growth rate of 0.123 and oscillating with a circular frequency of $4.94 rad/s$. This mode is plotted along with the spectrum and it can be seen that this mode also overlaps with the unstable eigenvalue from the eigenanalysis.

The eigenanalysis not only generates the eigenvalues but also the eigenvectors associated with each eigenvalue. For the unstable mode, the real part of the density, x/y momentum and energy component of the unstable eigenvector is shown in Fig.5.

B. Rotating stall for an axial compressor (NASA Rotor 67)

NutsCFD is used to analyze the performance of the first stage rotor (NASA Rotor 67) of a two stage transonic fan designed and tested at the NASA Glenn center [1]. Its design pressure ratio is 1.63, at a mass flow rate of 33.25 kg/sec.
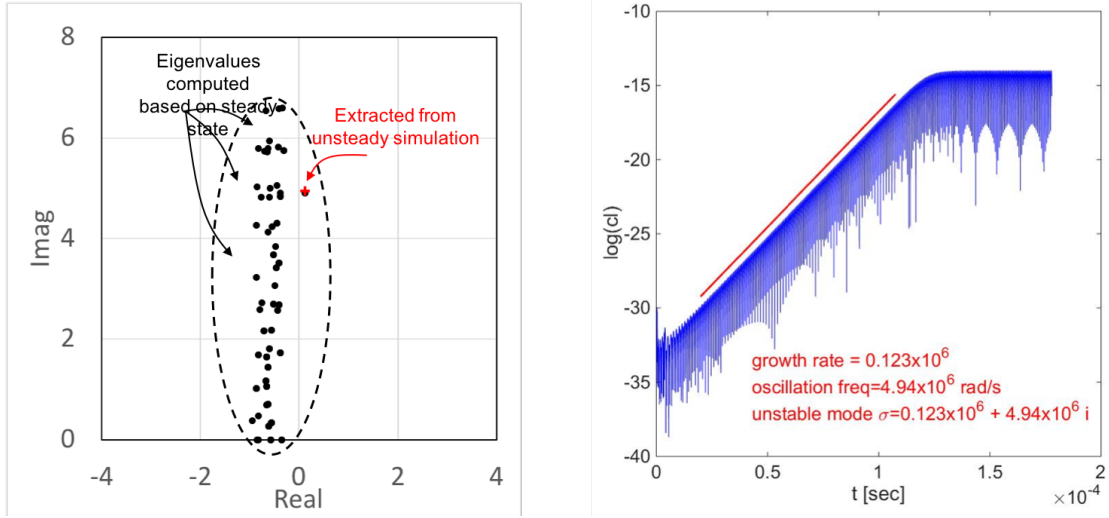
Fig. 4 Eigenspectrum from the steady state eigenvalue analysis compared with the linearly destabiling unsteady simulation for $Re = 55$**.**
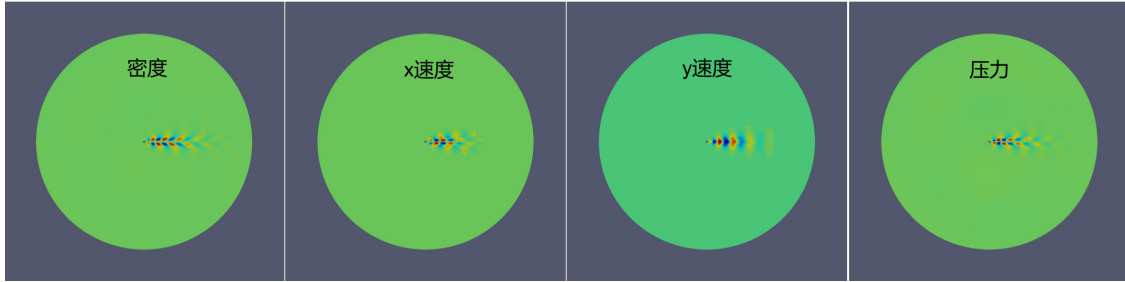
Fig. 5 Real part of the density, x/y momentum, energy components of the unstable eigenmode for $Re = 55$**.**

The NASA Rotor 67 has 22 blades with tip radii of 25.7 cm and 24.25 cm at the leading and trailing edge, respectively, and a constant tip clearance of 1.0 mm. The hub to tip radius ratio is 0.375 at the leading edge (TC = 0.6% span) and 0.478 at the trailing edge (TC = 0.75% span). The design rotational speed is 16,043 RPM, and the tip leading edge speed is 429 m/s with a tip relative Mach number of 1.38.
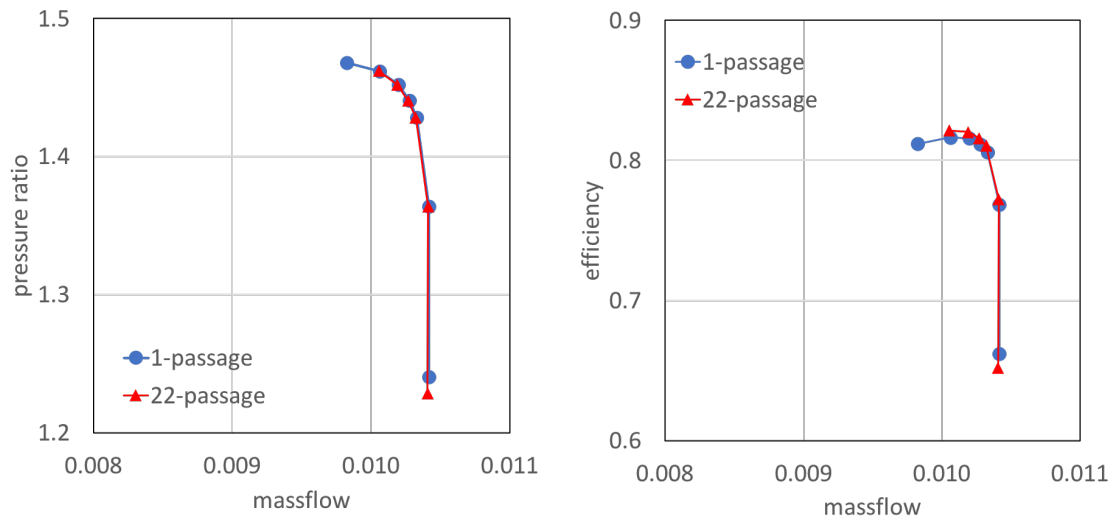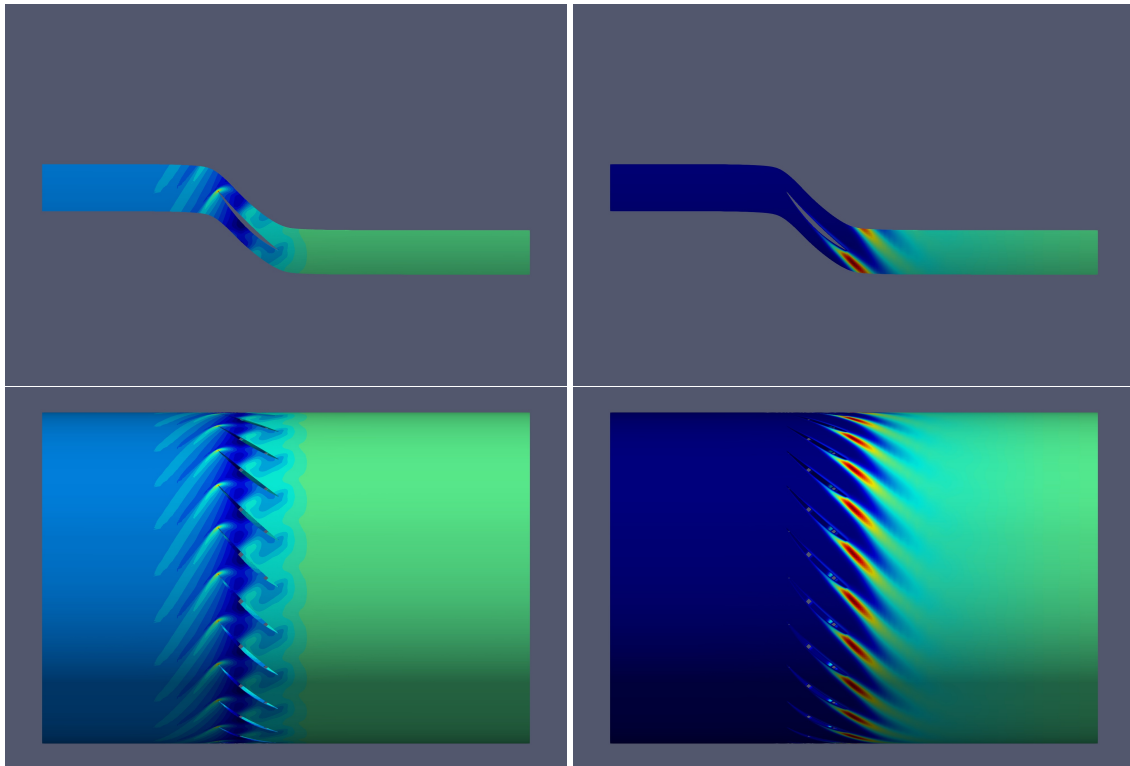
C. performance curve

V. Conclusion

Acknowledgements

References

[1] Strazisar, A. J., Wood, J. R., Hathaway, M. D., and Suder, K. L., "Laser anemometer measurements in a transonic axial-flow fan rotor," 1989.

Fig. 6 Q3D performance for rotor67 at 50% blade height with either single passage or whole annulus (22 passages).

Fig. 7 Q3D performance for rotor67 at 50% blade height with either single passage or whole annulus (22 passages).
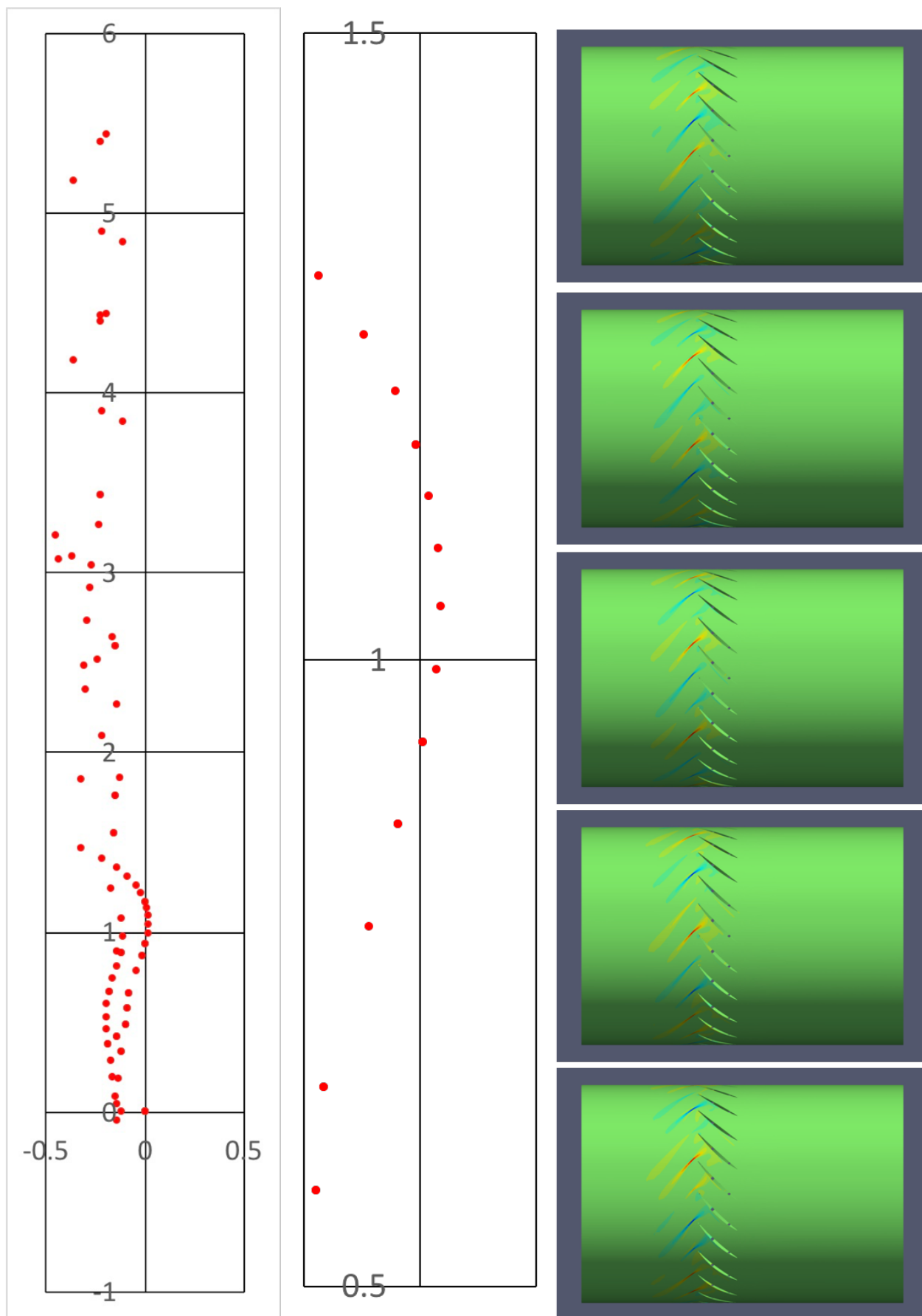
Fig. 8   18kpa eigenvalue.